



HAL
open science

Salinity effect on the compaction behaviour, matric suction, stiffness and microstructure of a silty soil

Zi Ying, Yu-Jun Cui, Nadia Benahmed, Myriam Duc

► To cite this version:

Zi Ying, Yu-Jun Cui, Nadia Benahmed, Myriam Duc. Salinity effect on the compaction behaviour, matric suction, stiffness and microstructure of a silty soil. *Journal of Rock Mechanics and Geotechnical Engineering*, 2021, 13 (4), pp.855-863. 10.1016/j.jrmge.2021.01.002 . hal-03602922

HAL Id: hal-03602922

<https://enpc.hal.science/hal-03602922>

Submitted on 9 Mar 2022

HAL is a multi-disciplinary open access archive for the deposit and dissemination of scientific research documents, whether they are published or not. The documents may come from teaching and research institutions in France or abroad, or from public or private research centers.

L'archive ouverte pluridisciplinaire **HAL**, est destinée au dépôt et à la diffusion de documents scientifiques de niveau recherche, publiés ou non, émanant des établissements d'enseignement et de recherche français ou étrangers, des laboratoires publics ou privés.

Salinity effect on the compaction behaviour, matric suction, stiffness and microstructure of a silty soil

Zi Ying¹, Yu-Jun Cui¹, Nadia Benahmed², Myriam Duc³

¹: Ecole des Ponts ParisTech, Laboratoire Navier/CERMES, 6-8 av. Blaise Pascal, Cité Descartes, Champs-sur-Marne, 77455 Marne-la-Vallée cedex 2, France

²: INRAE, Aix Marseille Univ, RECOVER, Equipe G2DR, 3275 route Cézanne, CS 40061, 13182 Aix-en-Provence, France

³: Université Gustave Eiffel, IFSTTAR/GERS/SRO, 14-20 boulevard Newton, Champs-sur-Marne, 77447 Marne-la-Vallée, France

Corresponding author:

Prof. Yu-Jun CUI
Ecole des Ponts ParisTech
6-8 av. Blaise Pascal, Cité Descartes, Champs-sur-Marne
77455 Marne-la-Vallée cedex
France

Telephone: +33 1 64 15 35 50

Fax: +33 1 64 15 35 62

E-mail: yu-jun.cui@enpc.fr

Abstract:

To better understand the salinity effect on the compaction behaviour of soil, standard Proctor compaction test was conducted on soil samples with different salinities. Matric suction and small strain shear modulus, G_{max} , were determined and pore size distribution was also investigated on samples statically compacted at different water contents. Results showed that with the decrease of soil salinity from initial value of 2.10‰ (g of salt/ kg of dry soil) to zero, the maximum dry density increased and the optimum water content decreased, whereas there was no significant change with the increase of soil salinity from 2.10‰ to 6.76‰. Interestingly, it was observed that, G_{max} also decreased when the soil salinity decreased from initial value of 2.10‰ to zero and kept almost constant when the soil salinity increased from 2.10‰ to 6.76‰, for dry samples with similar matric suction and also for samples compacted at optimum and on wet side whose matric suctions were slightly different due to the difference in remolded water content. Furthermore, the effect of salinity on compaction behaviour and G_{max} decreased for samples compacted from dry side to wet side. The pore size distribution exhibited bi-modal characteristics with two populations of micro-pores and macro-pores not only for samples compacted on dry side and at optimum state, but also for those compacted on wet side. Further examination showed that the modal size of micro-pores shifted to lower values and that of macro-pores shifted to higher values for saline soil compared to the soil without salt.

Keywords: silts; compaction; suction; stiffness; microstructure

1. Introduction

For the economic and environmental reasons, it is recommended to use local soils in geotechnical and geo-environmental constructions such as subgrades, dikes, dams and municipal waste barriers. In coastal area, soil pore water normally contains certain salinity, which can greatly affect the compaction behaviour of soils. Liu and Zhang (2014) reported that both the maximum dry density and optimum water content decreased with increasing salinity for saline soils with 3% ~ 8% clay-size fraction. Nevertheless, Ajalloeian et al. (2013) indicated that salinity had negligible effect on the compaction behaviour of fine-grained soils with 28% clay-size fraction. Abdullah et al. (1997, 1999) stated that the salt solution led to an increase in maximum dry density and a reduction of optimum water content for highly plastic clay whose main minerals were illite and smectite. The same observations were made on clayey soils with 48% clay minerals consisting of montmorillonite, polygorskite and kaolinite (Abood et al., 2007) and on expansive soils (Shariatmadari et al., 2011; Durotoye et al., 2016). They attributed this phenomenon to the decrease of diffused double layer thickness and the more oriented face-to-face clay particle contacts with the increase of salinity. From these studies, it appears that the salinity had different effect on compaction properties for soils with different clay fractions and mineral compositions. On the whole, the maximum dry density increased and the optimum water content decreased with increasing salinity for clays which had high clay fraction and swelling minerals, whereas the salinity had no significant effect on compaction behaviour or led to a reduction of both maximum dry density and optimum water content for soils with low clay fraction.

Salt can also significantly influence the strength or stiffness of compacted soils. Recent studies mainly focused on the strength variations with salinity changes (Abood et al., 2007; Ajalloeian et al., 2013; Zhang et al., 2013a; Carteret et al., 2014; Liu and Zhang, 2014). Some studies focused on the effect of salinity on the stiffness of illite (Witteveen et al., 2013) and cemented soils (Truong et al., 2012; Zhang et al., 2013b). It was reported that the unconfined compressive strength increased with increasing salinity for soils with a fraction of clay minerals as large as 48% (Abood et al., 2007) and for saline soils with only 3% ~ 8% clay-size fraction (Liu and Zhang, 2014). Liu and Zhang (2014) explained that the increased shear strength for saline soils was due to the salt crystal cementation of soil particles which improved soil mechanical behaviour. As for the samples with high quantity of clay minerals, the thickness of diffused double layer decreased with increasing salinity and this, in turn, caused repulsive force diminution and net attractive force increase (Mitchell and Soga, 2005; Israelachvili, 2011). The

increased net attractive force enabled soil particles to associate with each other in an aggregated manner, which may enhance soil strength (Moore, 1991; Di Maio et al., 2004; Tiwari et al., 2005; Abood et al., 2007). In addition to salinity effect, it was also reported that the stiffness of soil increased with the increase of matric suction but at a declining rate (Ng and Yung, 2008; Ng et al., 2009; Heitor et al., 2013). However, salinity had no significant effect on matric suction which was related to the capillary and hydration forces (Miller and Nelson, 1993; Leong et al., 2007; Sreedeeep and Singh, 2011).

Concerning the correlations between microstructure and mechanical behaviour, several studies focused on the salinity effect on microstructure variations. Carteret et al. (2014) performed scanning electron microscope (SEM) and mercury intrusion porosimetry (MIP) tests on compacted saline samples with different salinities. They observed that the salt crystallization of highly saline samples caused reduction of macro-pores and increase of meso-pores and micro-pores, and these salt crystals were found to form bonds among soil particles which led to the increase of soil strength. Zhang et al. (2013a) also observed some salt bonding between clay particles of loess on SEM images, and this bonding resulted in aggregation of particles, increasing the shear strength. Sarkar and Siddiqua (2016) conducted X-ray computed tomography (X-ray CT) test on bentonite-sand materials prepared by distilled water and salt solutions, and highlighted the salt effect on pore size distribution properties of compacted samples: the pore size and number of interconnected pores increased with increasing salinity due to the reduction of diffused double layer thickness.

It appears from the above-mentioned studies that the salinity effect on either compaction behaviour or matric suction or stiffness or microstructure was conducted on different soils. However, there were few studies focusing on all these different properties of a given soil. In this study, standard Proctor compaction test was first conducted on soil samples with different salinities. To further understand the salinity effect on soil compaction behaviour, filter paper method, bender element test and MIP test were carried out on samples compacted on dry side, at optimum and on wet side. Results allowed the coupled compaction behaviour, matric suction, stiffness and microstructure to be analysed.

2. Materials and methods

2.1 Tested materials

Natural saline silty soil was taken from Salin-de-Giraud, a traditional salt exploitation site in France. Its geotechnical properties are reported in Table 1. Fig. 1 shows the grain size distribution of the soil, which was determined by the dry sieving method for particles larger than 80 μm and by the hydrometer method for particles smaller than 80 μm , according to the French standards NF P94-056 (1996) and NF P 94-057 (1992), respectively. This soil consists of 20% sand, 63% silt-size particles (0.002 ~ 0.075 mm) and 17% clay-size fraction (< 0.002 mm). The main minerals, identified by XRD analysis, are quartz (39%), calcite (35%), feldspar (9.5%), illite (10.8%), chlorite (3.6%), kaolinite (1.3%) and NaCl crystallized on halite form (0.8%). The quantity of clay minerals (illite, chlorite and kaolinite) is 15.7%, in agreement with the clay-size fraction of 17% observed on grain size distribution curve.

Table 1. Geotechnical properties of the tested soil.

Property	Value
Specific gravity, G_s	2.72
Liquid limit, w_L (%)	29
Plastic limit, w_p (%)	19
Plasticity Index, I_p	10
VBS (g/100g)	0.98
Specif. surf. Area, SSA(m^2/g)	24.0

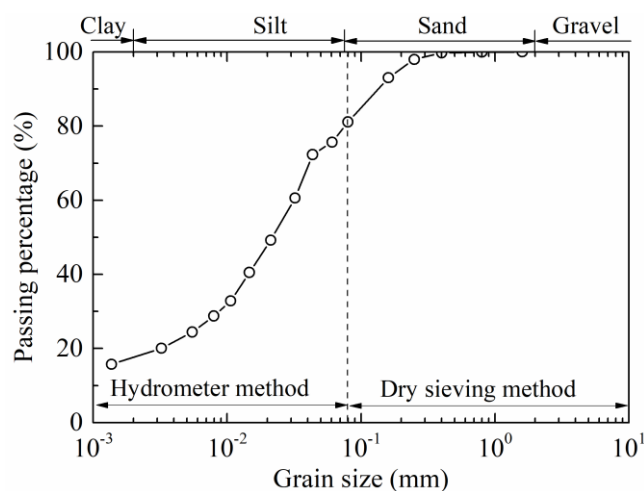


Fig. 1. Grain size distribution of natural soil.

Soil solutions were extracted by centrifugation method after several cycles of washing. The chemical compositions and ion concentration of soil solution extracts were determined by Inductively Coupled Plasma/Atomic Emission Spectroscopy (ICP/AES). As listed in Table 2, the ion concentration of soil solution extracts was transformed to ion concentration of soil pore water according to the dilution ratio. The salt concentration of soil pore water was estimated at about 13.3 g/L. Since the salt concentration of soil pore water always changed with water content variations, the soil salinity, defined as the ratio of salt mass to dry soil mass, was adopted in this study. For the tested soil, the soil salinity was found to be 2.1‰ (g of salt/kg of dry soil).

Table 2. Chemical analysis of natural soil pore water.

Solution	Chemical compositions (mg/L) – ICP/AES method								Salt concentration, <i>c</i> (g/L)	Soil salinity, <i>r'</i> (‰ or g salt/kg of dry soil)
	Cl	Na	Ca	K	Mg	Fe	Al	Si		
Soil pore water	7521	5096	215	225	176	18	7	39	13.3	2.1

2.2 Soil salinity adjustment

Since the main ion species of soil pore water were Cl^- , Na^+ , Ca^{2+} , K^+ , and Mg^{2+} , the same as the ion compositions of synthetic sea water (French standard NF P 18-837, 1993, as listed in Table 3), five different salts of synthetic sea water were chosen for preparing the mixed salt solution to be added to the natural saline soil in order to obtain salted soil with higher salinity. The quantity of additive salt was determined according to the initial salinity of natural saline soil and the target salinity of salted soil (Ying et al., 2020a). The total additive salt mass was adjusted to each salt mass according to the proportions of the five different salts in synthetic sea water. Mixed salt solution was prepared by dissolving the five additive salts in deionized water. Afterwards, salt solution was sprayed to natural soil in layers to reach the desired soil salinities of about 4.83‰ (or g of salt/kg of dry soil) and 6.76‰ (or g of salt/kg of dry soil), respectively. Note that the maximum target soil salinity of 6.76‰ corresponded to the salt concentration of soil pore water of 35 g/L (salt concentration of synthetic sea water) for salted soil at 20% water content.

Table 3. Chemical compositions of synthetic sea water.

salts	NaCl	MgCl ₂ ·6H ₂ O	MgSO ₄ ·7H ₂ O	CaSO ₄ ·2H ₂ O	KHCO ₃
Salt mass (g) in 1000 g deionized water	30.0	6.0	5.0	1.5	0.2
Percentage (%)	70.26	14.05	11.71	3.51	0.47

To decrease the salinity of natural saline soil, leaching tests were carried out. Leaching column was filled with natural soil. Then, deionized water, with a water head of 1 m, was flushed through the column from bottom to top in order to remove the initial salt (Fig. 2). The water flow rate was controlled to be lower than 0.3 mL/s, preventing the migration of fine particles and avoiding the destruction of soil aggregates. To minimise as much as possible the soil disturbance during leaching, a layer of gravel, geotextile and filter paper were placed on the top and bottom surface of the soil. The effluent was collected and electrical conductivity (EC) was measured to verify whether the salt was washed out. The leaching of soil was repeated until the amount of salt, thus the EC, was reduced considerably. When the electrical conductivity of leaching water was close to the one of deionized water and kept almost constant, the test was stopped and a small quantity of leached soil was taken out to verify the final soil salinity. A value as low as 0.05‰ (or g of salt/kg of dry soil) was obtained, which could be regarded as zero. The natural soil, salted soil and leached soil were then air-dried, ground and sieved through 5 mm mesh. The larger soil particles which could not pass through the 5 mm sieve were ground again and rescreened until the whole soils passed through the sieve (Tang et al., 2011).

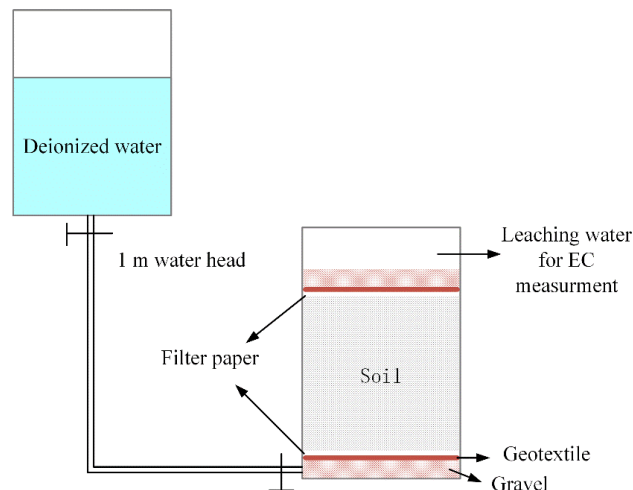


Fig. 2. Sketch of the equipment for salt leaching experiment.

2.3 Sample preparation

Air-dried soil was humidified by spraying deionized water to reach different target water contents on dry side, wet side and at optimum, and then stored in sealed plastic bag for 24 h aiming at salt and water homogenization. Afterwards, the samples were reconstituted either by dynamic compaction for proctor test or by static compaction for the matric suction and small strains shear modulus measurements as well as for the microstructure investigation. For these cases of static compaction, the samples were reconstituted at the target dry density using double pistons acting at the top and bottom of the soil samples to ensure uniform distribution of stresses inside the sample, hence, a better soil homogeneity with respect to the dry density (Cui and Delage, 1996). The samples for matric suction measurement and MIP test had a dimension of 50 mm diameter and 20 mm height, and the samples for small strain shear modulus measurement had 50 mm in diameter and 50 mm in length.

2.4 Proctor compaction test

Standard Proctor compaction tests were conducted following the French standard NF P94-093 (1999). Air-dried soil was prepared with the procedure presented previously. Deionized water was then added into the soil to reach different water contents. At each water content, the soil was dynamically compacted in three layers into proctor mould, with 25 blows of the hammer for each layer. The compacted sample was trimmed by means of a straightedge scraping across the top of the mould. The density of compacted sample (ρ) was then determined considering the sample mass and the mould volume. A portion of sample was taken for water content determination.

When a salted sample was dried in an oven, the water evaporated but the salt remained with dry soil (Noorany, 1984). Thus, the water content (w) computed from the conventional equation (Eq. 1) was not equal to the water content (w') of saline soil which was the ratio of salty water mass (m_{sw}) to dry soil mass (m_s):

$$w = \frac{m_w}{m_d} \quad (1)$$

where m_w is the pure water mass and m_d is the solid mass after oven-drying which contained total mass of soil and salt.

The water content (w') of saline soil should be calculated by Eq. 2 taking the dissolved salt into

account (Noorany, 1984; ASTM D4542-95, 2001; Ying et al., 2020a):

$$w' = \frac{m_{sw}}{m_s} = \frac{m - m_d}{m_d - rm} \quad (2)$$

where r is the water salinity, expressed as the mass ratio of salt to salty water.

To convert the salinity on the soil basis to the solution basis, the following equation was adopted (Reitemeier, 1946; Ying et al., 2020a):

$$r = \frac{r'}{w'} \quad (3)$$

where r' is the soil salinity on the basis of dry soil mass.

Then, the dry density (ρ_d) for saltless soil can be calculated using Eq. 4:

$$\rho_d = \frac{\rho}{1+w} \quad (4)$$

However, for saline soil, the dry density calculated by Eq. 4 was overestimated because of the consideration of the dissolved salt as soil solids. Thus, the dry density of saline soil should be calculated by Eq. 5 (Noorany, 1984; ASTM D4542-95, 2001; Siddiqua et al., 2011):

$$\rho_d' = \frac{\rho}{1+w'} \quad (5)$$

The saturation degree (S_r) of compacted samples can be determined from the water content and dry density by Eq. 6:

$$S_r = \frac{w \cdot \rho_d \cdot G_s}{\rho_w \cdot G_s - \rho_d} = \frac{w \cdot G_s}{\rho_w (G_s / \rho_d - 1)} \quad (6)$$

where G_s is the specific gravity; ρ_w is the liquid density.

Finally, based on the values of dry density and water content, the proctor compaction curves of saltless soil and saline soil with different soil salinities were plotted. The compaction states at dry and wet sides of optimum and at optimum water content with target dry densities were selected to prepare samples for matric suction, small strain shear modulus and microstructure investigations.

2.5 Matric suction measurement

Matric suction of soil sample was determined by filter paper method, according to ASTM

standard D 5298-10 (2010). Whatman No. 42 filter paper was oven-dried at least 16 h prior to use in the measurements. Three stacked filter papers were sandwiched between two soil samples. The central filter paper used for matric suction measurement was slightly smaller in diameter than the outer filter papers, preventing the central filter paper from direct contact with soil. The entire sandwiched samples were wrapped by plastic film and enveloped by scotch tape. Then, they were stored in a chamber at a relative humidity of 100% and a temperature of $20 \pm 2^\circ\text{C}$ to allow moisture equilibration for two weeks. After equilibration, the water contents of soil sample and central filter paper were measured.

According to ASTM standard (D5298-16, 2016), the following equations of Whatman No. 42 filter paper calibration curves were used to transform the water content of filter paper to matric suction of soil sample:

$$\log \psi_m = \begin{cases} 5.327 - 0.0779w_f & w_f \leq 45.3\% \\ 2.412 - 0.0135w_f & w_f > 45.3\% \end{cases} \quad (7)$$

where ψ_m is matric suction of soil sample (kPa), w_f is the water content of filter paper (%). Note that the mean value of matric suction and water content on the two replicated measurements was considered.

2.6 Bender element test

The bender element technique was used to measure the small strain shear modulus. The set-up of bender elements and a schematic diagram are shown in Fig. 3. This system consists of two piezo-ceramic bender elements, a function generator, an amplifier and an oscilloscope (Wang et al., 2017, 2020; Zhang et al., 2018).

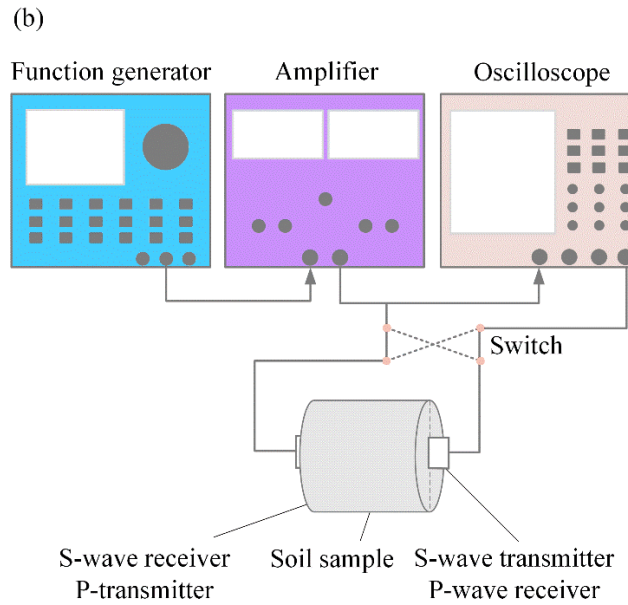
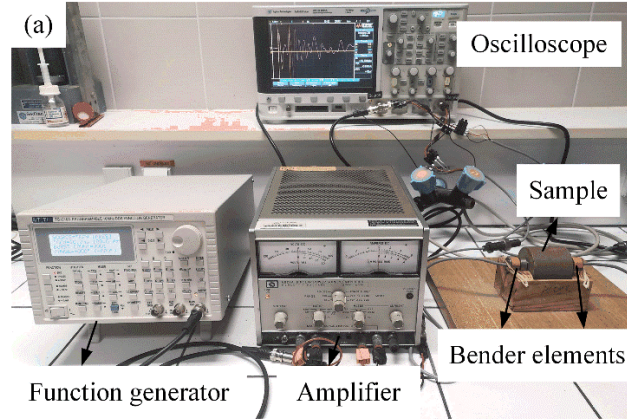


Fig. 3. Set-up of bender element test: (a) photo of the set-up; (b) sketch of the set-up (after Wang et al., 2017).

Immediately after compaction, the samples were carefully covered by paraffin to avoid water evaporation. Then, a slot was performed on the surface of the sample extremities with the same direction to install the piezo-ceramic elements and ensure a good contact with soil. The sample was then placed on a wooden holder for a good insulation and for avoiding any signal electrical perturbation (Fig. 3a). Hereafter, a simple pulse was generated by the function generator and amplified by the amplifier. The S+P method proposed by Wang et al. (2017) was adopted to determine the arrival time of shear wave (Δt). In the S+P method, both transmitted and received signals were captured by the oscilloscope through modifying the connection between the two benders (Fig. 3b). The shear wave velocity (v_s) was calculated by Eq. 8:

$$v_s = \frac{L_{tt}}{\Delta t} \quad (8)$$

where L_{tt} is the travel length or tip-to-tip distance between two bender elements.

Finally, the small strain shear modulus (G_{max}) was determined using Eq. 9:

$$G_{max} = \rho v_s^2 \quad (9)$$

where ρ is the density of soil sample. To check the reproducibility of tests, the G_{max} measurement was determined in duplicate. And the mean value was used in this study.

2.7 Microstructure investigation

Autopore IV 9500 mercury intrusion porosimeter was used to investigate the microstructure of compacted samples. After compaction, one small piece of soil was carefully cut from the sample, then frozen using liquid nitrogen under vacuum and dried using a freeze dryer for 24 h aiming at sublimation of frozen water. To perform the MIP test, the freeze-dried piece was firstly put into a low pressure system with a pressure range varying from 3.6 kPa to 200 kPa, then transferred to a high pressure system with the maximum pressure of 230 MPa. The corresponding detectable entrance pore diameter ranged from 0.006 μm to 350 μm .

3. Results

3.1 Proctor compaction behaviour

The results of the proctor compaction curves for soil without salt and those with different soil salinities are depicted in Fig. 4. It can be observed that, with decreasing soil salinity from initial value of 2.10‰ to zero, the compaction curve moved upwards and leftwards, implying that the saltless soil had higher maximum dry density and lower optimum water content than that of natural soil with soil salinity of 2.10‰. However, as soil salinity increased from 2.10‰ to 4.83‰ and 6.76‰, the compaction curves did not exhibit distinguishable changes: the saline soil samples with different salinities had rather close values of maximum dry densities and optimum water contents. Comparison between proctor compaction curves of saltless soil and those of saline soils suggested that the salt had more significant effect on the compaction curves on dry side than that on wet side.

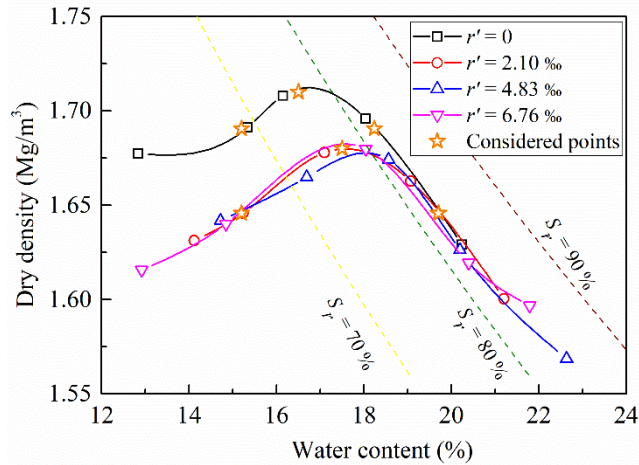


Fig. 4. Salinity effect on proctor compaction behaviour.

The properties of the compacted samples used for matric suction, small strain shear modulus and microstructure investigations are given in Table 4. The corresponding points are shown in Fig. 4. All the considered compaction states were located on the proctor compaction curves. Note that the same compaction pressure of about 2200 kPa was recorded for all samples. Note also that for a given soil salinity, the chosen points on dry and wet sides corresponded to the same dry density. The corresponding compactness which was the ratio of target dry density to maximum dry density, were 98.8% for soil without salt and 98.2% for soils with soil salinities of 2.10‰ and 6.76‰ that were almost similar.

Table 4. Properties of compacted samples.

Sample	$r' = 0$			$r' = 2.10\text{‰}$ and $r' = 6.76\text{‰}$		
	Dry side	Optimum	Wet side	Dry side	Optimum	Wet side
Water content (%)	15.2	16.5	18.2	15.2	17.5	19.7
Dry density (Mg/m ³)	1.69	1.71	1.69	1.65	1.68	1.65
Degree of saturation (%)	68	76	82	63	77	82
Compactness (%)	98.8	100	98.8	98.2	100	98.2

3.2 Matric suction

Figure 5 depicts the changes in matric suction of compacted samples on dry side, wet side and at optimum. It appears that all the points lay on one unique line, suggesting that the matric suction was highly related to the water content of samples, whereas the salinity had no significant effect on matric suction. This was in good agreement with previous results from

Miller and Nelson (1993), Leong et al. (2007), Sreedeeep and Singh (2011) and Zhang et al. (2017). It was also observed that, for the dry samples with the same water content, the matric suctions of saltless and saline samples were quite close, while the matric suctions of saltless samples compacted at optimum and on wet side were noticeably higher than those of saline samples with soil salinity of 2.10‰ and 6.76‰.

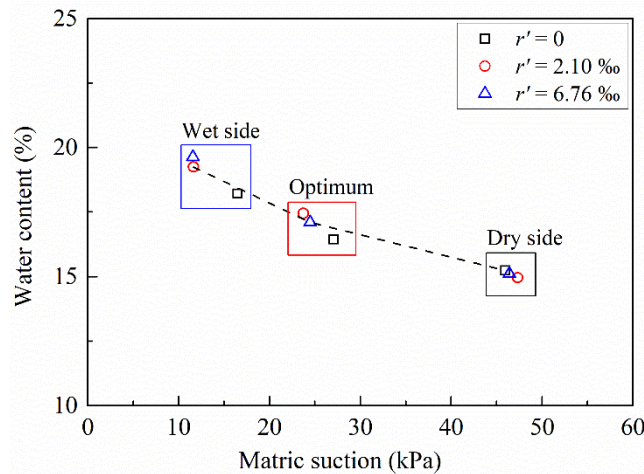


Fig. 5. Matric suction of compacted samples at dry side, wet side and optimum state.

3.3 Small strain shear modulus

The G_{max} was affected by many factors, including soil properties, compaction state, compaction stress and matric suction (Ng et al., 2009). As shown in Table 4, the compactness was almost the same for samples having different salinities which were compacted at dry, optimum and wet sides respectively, although the dry density of saltless samples was higher than that of saline samples. Moreover, as mentioned before, all samples were subjected to the same compaction pressure of around 2200 kPa. This implied that the effects of compactness (or dry density) and compaction energy on G_{max} can be ignored. Thus, there were remaining two factors affecting the G_{max} values: one was matric suction, and the other one was salinity. The variations of G_{max} with soil salinity are plotted in Fig. 6. For the samples compacted on the dry side, the matric suction was rather close (Fig. 5). Thus, the soil salinity was the sole factor to influence the G_{max} for the dry samples. As shown in Fig. 6, the G_{max} for dry samples decreased with the decrease of soil salinity from initial value of 2.10‰ to zero, whereas it kept almost constant with the increase of soil salinity from 2.10‰ to 6.76‰. The same trend of G_{max} variations were also observed for the samples compacted at optimum and wet side. However, in that case, the difference of G_{max} between the saltless samples and the saline samples was controlled by both

matric suction and soil salinity. For the samples compacted at optimum and on wet side, the matric suctions for saltless samples were higher than those of samples with soil salinities of 2.10‰ and 6.76‰ (Fig. 5). Ng et al. (2008, 2017) and Heitor et al. (2013) indicated that the G_{max} increased with increasing matric suction. This implies that, if the salinity effect was neglected, the G_{max} for the saltless samples should be higher than those of samples with soil salinity of 2.10‰ and 6.76‰, due to their higher matric suction. Nevertheless, it was observed that G_{max} for the samples compacted at optimum and on wet side decreased with the decrease of soil salinity from 2.10‰ to zero, suggesting that the decrease of salinity led a reduction of G_{max} that prevailed the increase of G_{max} as matric suction increased. This resulted in a decrease of salinity effect on G_{max} from dry side to wet side, due to the balance of the increase of G_{max} with increasing matric suction and the decrease of G_{max} with decreasing salinity for optimum and wet side samples. Specifically, as soil salinity decreased from 2.10‰ to zero, the G_{max} decreased from 27.24 MPa to 23.45 MPa (14%) for samples compacted on dry side, from 23.44 MPa to 20.80 MPa (11%) for samples compacted at optimum, and from 20.13 MPa to 19.32 MPa (4%) for samples compacted on wet side. This salinity effect on G_{max} was in full agreement with the changes of compaction curves observed previously - the salinity effect on compaction curves also decreased from dry side to wet side (Fig. 4).

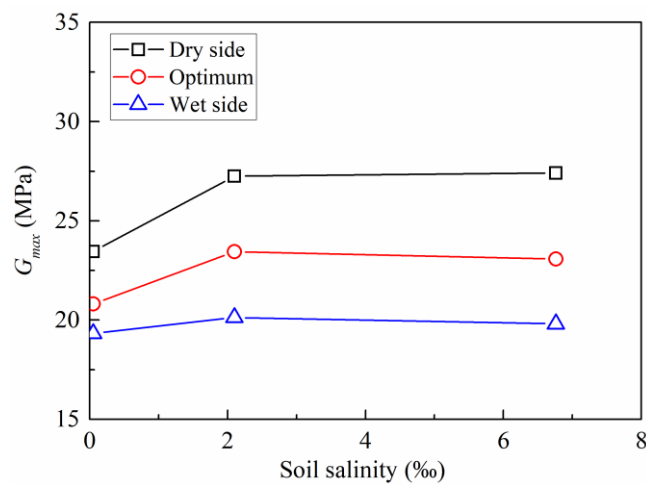


Fig. 6. Salinity effect on small strain shear modulus.

3.4 Microstructure investigation

The cumulative curves and corresponding derived curves are presented in Fig. 7 for the samples compacted on dry side, Fig. 8 for the samples compacted at optimum and Fig. 9 for the samples compacted on wet side. Based on the MIP results and the hypothesis that the water is contained

in small pores (Wan *et al.*, 1995; Romero *et al.*, 2011), the water ratio (i.e. void ratio of water-saturated pores, $e_w = wG_s$, where w is water content and G_s is specific gravity) and delimiting diameter between water-saturated pores and dry pores were determined, as shown in Figs. 7a, 8a and 9a. The corresponding distribution of water-saturated pores are presented in Figs. 7b, 8b and 9b. It appears from the cumulative curves that, the total intruded void ratios were relatively close to the initial void ratio of samples which were determined from sample dimension. The total intruded void ratios were almost similar for dry samples having different salinities. Concerning the optimum and wet samples, the total intruded void ratios of saltless samples were slightly lower than that of saline samples, which might be due to its relative higher dry density of saltless samples. As shown in Figs. 7b, 8b and 9b, the derived curves exhibited typical bi-modal characteristics not only for the samples compacted at dry side and optimum as usually observed, but also for the samples compacted wet of optimum, with a population of micro-pores and a population of macro-pores. For all samples on dry side, at optimum and on wet side, the water was mostly adsorbed and held in the micro-pores, leaving the most of macro-pores being dry. As for the dry samples, with decreasing soil salinity from the initial value of 2.10‰ to zero, the modal size of micro-pores increased from 0.63 μm to 0.78 μm and that of macro pores decreased from 11.63 μm to 10.23 μm , while there was no significant change when the soil salinity increased from 2.10‰ to higher value of 6.76‰ (Fig. 7b). The similar results were obtained on the samples compacted at optimum: as the soil salinity decreased from 2.10‰ to zero, the modal size of micro-pores shifted from 0.91 μm to 1.03 μm and that of macro-pores shifted from 13.17 μm to 10.86 μm , whereas the modal sizes of both macro-pores and micro-pores had no significant change with increasing soil salinity to 6.76‰ (Fig. 8b). As for the wet samples, the modal size of micro-pores increased from 0.91 μm to 1.05 μm and that of macro-pores decreased from 12.91 μm to 11.82 μm with decreasing soil salinity from 2.10‰ to zero, while the modal size of micro-pores decreased slightly and that of macro-pores increased with increasing soil salinity from initial value of 2.10‰ to 6.76‰ (Fig. 9b). Besides, as salinity increased, an increase in the frequency of macro-pores was observed on all kinds of samples.

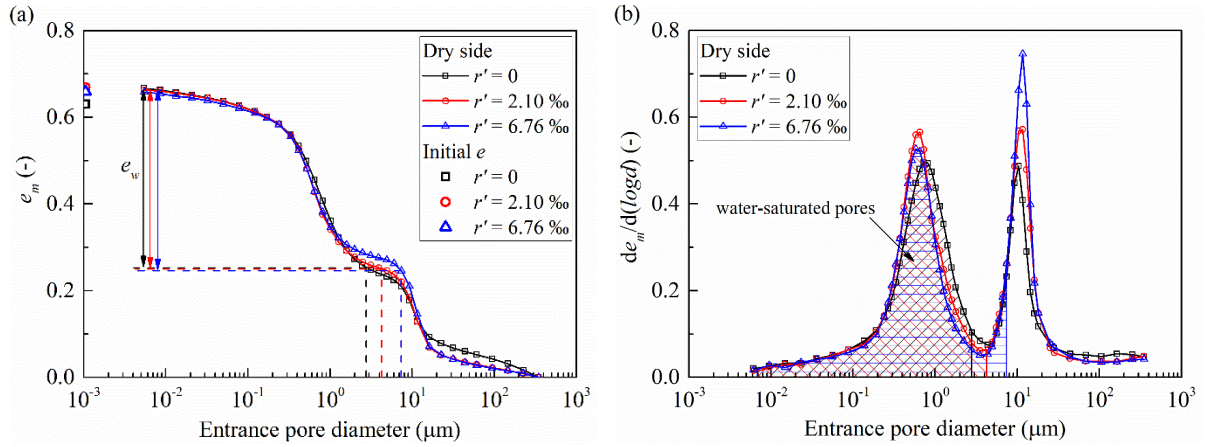


Fig. 7. MIP results of samples compacted on dry side: (a) cumulative intrusion curves; (b) derived curves.

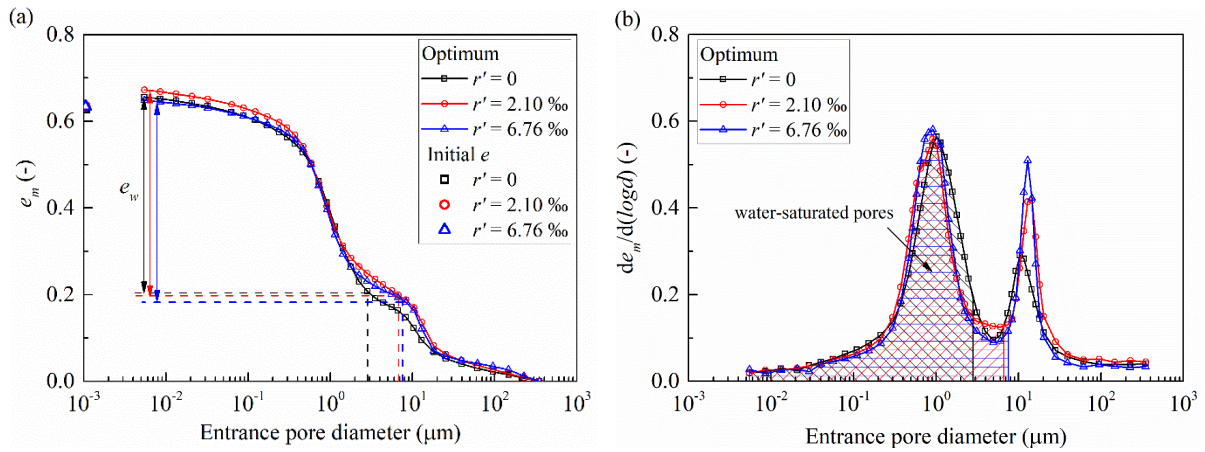


Fig. 8. MIP results of samples compacted at optimum water content: (a) cumulative intrusion curves; (b) derived curves.

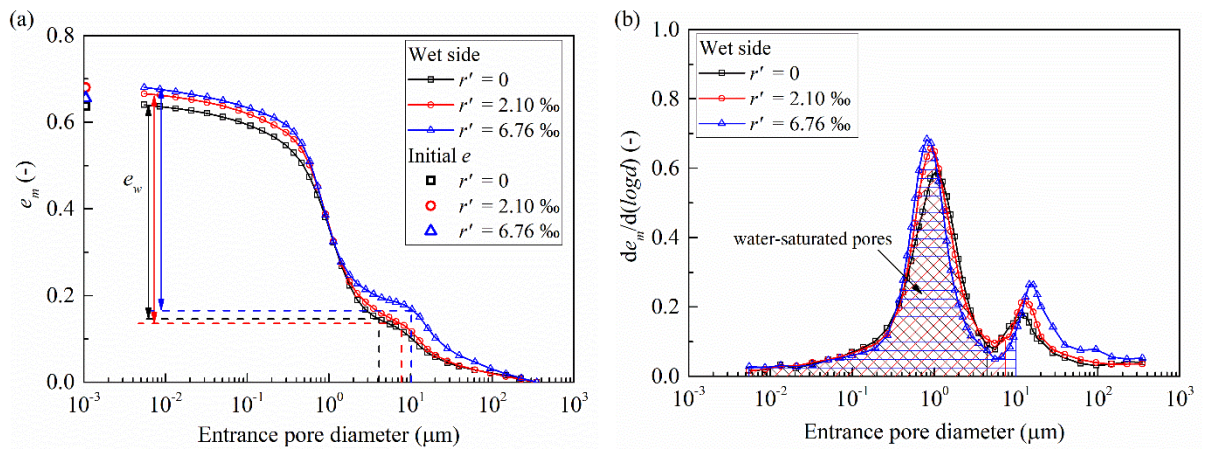


Fig. 9. MIP results of samples compacted on wet side: (a) cumulative intrusion curves; (b) derived curves.

4. Discussion

Microstructure of compacted soil was significantly dependent on the compacted water content (Delage et al., 1996). For silty soil, on dry side, the clay coated the surface of grains and the compaction cannot significantly deform the aggregates due to the high suction effect. This led to an aggregated structure characterised by bi-modal pore size distributions. On wet side, the clay fraction formed a continuous or more compact matrix around the sand or silt grains and the clay paste was able to fill the macro-pores. In that case, a uni-modal pore population was usually identified. Thus, it was not a common result that the wet samples presented aggregated structure with a high population of micro-pores and a small population of macro-pores, as shown in Fig. 9b. Russo and Modoni (2013) also observed the bi-modal pore size distribution characteristics for alluvial silty sand with only 13% clay-size fraction which was compacted on wet side. Burton et al. (2014) indicated that the wet samples can also present aggregated structure if their compaction energy and degree of saturation were low. For the tested silty soil, the clay-size fraction was only 17%. The degree of saturation of compacted samples was around 82% that was close to the value at optimum state (78%). Thus, the low clay fraction and the degree of saturation close to the one at optimum might be the possible reasons for the bi-modal pores size distribution characteristics observed on wet samples that the limited clay paste could not form a continuous matrix to fill all macro-pores.

As observed in Figs. 7b, 8b and 9b, the modal size of micro-pores decreased, while the modal size and frequency of macro-pores increased with increasing soil salinity from zero to 2.10‰ and 6.76‰. The changes in micro-pores were mainly attributed to the salinity effect which led to a decrease of diffused double layer thickness of clay minerals (Ravi and Rao, 2013; Thyagaraj and Salini, 2015). The microstructure of compacted silty soil was characterised by sand or silt grain skeleton with clay particles coating these grains, and these grains and clay particles formed aggregates (Delage et al., 1996; Lemaire et al., 2013). The pores within these aggregates were identified as micro-pores and the pores between these aggregates were regarded as macro-pores. As salinity increased, the thickness of diffused double layer decreased (Sridharan and Jayadeva, 1982; Sridharan and Prakash, 2000), leading to a reduction of micro-pore size for clay particles. Such decrease of diffused double layer thickness further induced an increase of macro-pore size and its frequency (Yılmaz et al., 2008; Shariatmadari et al., 2011). In addition, the frequency of macro-pores was also affected by the dry density: the higher the dry density, the lower the frequency of the macro-pores (Romero, 2013). It was noting that the salinity effect on the pore size distributions (especially for micro-pores) were visible with

increasing salinity from zero to 2.10‰, while this salinity effect was negligible when the salinity increased from 2.10‰ to 6.76‰. This might be attributed to the low clay fraction and its less active clay minerals (10.8 % illite, 3.6% chlorite and 1.3% kaolinite) in the tested silty soil limiting the compression of diffused double layer at higher salinity (Ying et al., 2020b), as its thickness already decreased significantly at 2.10‰ soil salinity. As most water was contained in the micro-pores, the relationship between water content and matric suction was mainly governed by the micro-pores while the dry macro-pores which were easily affected by dry density played a negligible role. Thus, the points of water content and matric suction converged to one unique line despite the different dry densities (Fig. 5). This was consistent with the results obtained by Heitor et al. (2013), showing that when the soil water retention properties of compacted silty sand were expressed in terms of water content and matric suction, the matric suctions were independent of dry density. The salinity effect on the matric suction was slight as observed in Fig. 5, which might be attributed to the visible but insignificant changes of micro-pores induced by salinity.

As soil microstructure changed with increasing salinity, the G_{max} of saline samples was expected to be higher than that of the samples without salt (Fig. 6). Since the distance between interlayers of clay decreased with the reduction of diffused double layer thickness, the inter-particle repulsive forces decreased, resulting in an increase of net attractive forces which may make clay particles attract each other and agglomerate (Warkentin and Yong, 1962; Sridharan et al., 2002; Israelachvili, 2011). This association enhanced soil strength (Warkentin and Yong, 1962; Sridharan et al., 2002). As far as the compaction behaviour was concerned, for the same compaction energy, a stiffer soil with higher G_{max} presented higher resistance to compaction. As a result, a lower maximum dry density of saline samples was obtained (Fig. 4). Meanwhile, more water was needed to destroy soil aggregates for stiffer soils. Thus, the optimum water content increased for saline soil (Fig. 4). However, the optimum degree of saturation seemed to be insensitive to salinity (Table 4), even though the microstructure and stiffness varied. This was consistent with the observations made by Tatsuoka (2015) and Tatsuoka and Correia (2018). They reported that the optimum saturation degree of compacted soil was nearly 82%, independent of soil type and compaction energy level. It can be deduced from Eq. 6 that, for the saline soil, the balance between the increased optimum water content and the decreased maximum dry density led to a negligible change in optimum saturation degree.

Regarding the saline samples with different salinities, they had rather close G_{max} and proctor

compaction curves. It was consistent with the changes in microstructure that these behaviour varied significantly when the soil salinity increased from zero to 2.10‰, while these variations were slight with increasing soil salinity from 2.10‰ to 6.76‰, due to the limited salinity effect through changes of diffused double layer thickness at higher salinity. Similar observations were made by Ajalloeian et al. (2013): the shear strength and friction angle increased then kept almost constant with increasing salinity in soils with only 28% clay-size fraction. It was also comparable to the results of saturated bentonite whose residual shear strength increased significantly in the range from 0 to 0.5 mol/L NaCl solution then had negligible variations for concentrations larger than 0.5 mol/L (Di Maio, 1996).

5. Conclusions

To better understand the salinity effect on the compaction behaviour of silty soil, standard Proctor compaction test, filter paper method and bender element test coupled with mercury intrusion porosimetry test were conducted on a silty soil with different salinities. The obtained results allowed the following conclusions to be drawn:

(1) The pore size distribution curves presented bi-modal characteristics not only for the samples compacted at dry side and optimum state as usually observed but also for the samples compacted on wet side. The smaller quantity of macro-pores for wet samples can be attributed to the low clay-size fraction whose paste could not form a continuous matrix to fill all macro-pores, and to the degree of saturation close to that of optimum.

(2) The pore size distribution of compacted samples also depended on soil salinity. For the samples with soil salinities of 2.10‰ and 6.76‰, the modal size of micro-pores shifted to smaller values, whereas the modal size of macro-pores shifted to larger values than that of samples without salt. This can be explained by the decrease of diffused double layer thickness of clay particles, leading to a reduction of the modal size of micro-pores and further inducing an increase of the frequency and modal size of macro-pores.

(3) Due to the modification of microstructure associated to salinity, the samples with soil salinities of 2.10‰ and 6.76‰ exhibited higher G_{max} than that of samples without salt. This observation was not only made on dry samples with similar matric suctions, but also for the samples compacted at optimum and on wet side, whose matric suctions were slightly different, due to the difference in remolded water content. The higher G_{max} obtained for saline soil could

be explained by the fact that, as salinity increased, the net attractive forces increased with the reduction of diffused double layer thickness that made clay particles attract each other and agglomerate, giving rise to an increase of G_{max} .

(4) The saline soil exhibited higher G_{max} and became less compactible. Thus, for the same compaction energy, the saline soil exhibited lower maximum dry density and higher optimum water content. Besides, the effect of salinity on compaction behaviour and G_{max} decreased while passing from dry side to wet side.

(5) The proctor compaction curves and G_{max} of saline samples with different soil salinities were rather similar. This could be attributed to the low clay fraction and their mineral compositions (illite, chlorite and kaolinite), which limited the salinity effect through changes in diffused double layer thickness of clay particles.

Acknowledgements

The authors would like to thank the China Scholarship Council (CSC), Ecole des Ponts ParisTech (ENPC) and INRAE for their financial support.

References

- Abdullah WS, Alshibli KA, Al-Zou'bi MS. Influence of pore water chemistry on the swelling behaviour of compacted clays. *Appl Clay Sci* 1999;15(5-6):447-462.
- Abdullah WS, Al-Zou'bi MS, Alshibli KA. On the physicochemical aspects of compacted clay compressibility. *Can Geotech J* 1997;34(4):551-559.
- Abood TT, Kasa AB, Chik ZB. Stabilisation of silty clay soil using chloride compounds. *J Eng Sci Technol* 2007;2(1):102-110.
- Ajalloeian R, Mansouri H, Sadeghpour AH. Effect of saline water on geotechnical properties of fine-grained soil. *EJGE* 2013;18:1419-1434.
- ASTM D4542-95. Standard Test Method for Pore Water Extraction and Determination of the Soluble Salt Content of Soils by Refractometer. ASTM International, West Conshohocken, PA. 2001.
- ASTM D5298-16. Standard Test Method for Measurement of Soil Potential (Suction) Using Filter Paper. ASTM International, West Conshohocken, PA. 2016.
- Burton GJ, Sheng DC, Campbell C. Bimodal pore size distribution of a high-plasticity compacted clay. *Géotechnique Lett* 2014;4(2):88-93.
- Carteret Rd, Buzzzi O, Fityus S, Liu XF. Effect of naturally occurring salts on tensile and shear strength of sealed granular road pavements. *J. Mater Civ Eng* 2014;26(6):04014010.

- Cui YJ, Delage P. Yielding and plastic behaviour of an unsaturated compacted silt. *Géotechnique* 1996;46(2):291-311.
- Delage P, Audiguier M, Cui YJ, Howat MD. Microstructure of a compacted silt. *Can. Geotech J* 1996;33(1):150-158.
- Di Maio C. Exposure of bentonite to salt solution: osmotic and mechanical effects. *Géotechnique* 1996;46(4):695-707.
- Di Maio C, Santoli L, Schiavone P. Volume change behaviour of clays: the influence of mineral composition, pore fluid composition and stress state. *Mech Mater* 2004;36 (5-6):435-451.
- Durotoye TO, Akinmusuru JO, Ogbiye AS, Bamigboye GO. Effect of common salt on the engineering properties of expansive soil. *Int J Eng Technol* 2016;6(7):233-241.
- Heitor A, Indraratna B, Rujikiatkamjorn C. Laboratory study of small-strain behavior of a compacted silty sand. *Can Geotech J* 2013;50(2):179-188.
- Israelachvili JN. Intermolecular and surface forces, 3rd edition. Academic press. 2011.
- Lemaire K, Deneele D, Bonnet S, Legret M. Effects of lime and cement treatment on the physicochemical, microstructural and mechanical characteristics of a plastic silt. *Eng Geol* 2013;166:255-261.
- Leong EC, Widiastuti S, Lee CC, Rahardjo H. Accuracy of suction measurement. *Géotechnique* 2007;57(6):547-556.
- Liu JY, Zhang LJ. The microstructure characters of saline soil in Qarhan Salt Lake area and its behaviours of mechanics and compressive strength. *Arab J Sci Eng* 2014;39(12): 8649-8658.
- Miller DJ, Nelson JD. Osmotic suction as a valid stress state variable in unsaturated soil mechanics. *Unsaturated Soils ASCE* 1993:64-76.
- Mitchell JK, Soga K. Fundamentals of soil behaviour, 3rd edition. John Wiley & Sonc, Inc. 2005.
- Moore R. The chemical and mineralogical controls upon the residual strength of pure and natural clays. *Géotechnique* 1991;41(1):35-47.
- NF P 18-837. Standard for special products for hydraulic concrete construction-Hydraulic binder based needling and/or sealing products-Testing of resistance against seawater and/or water with high sulphate contents. 1993.
- NF P 94-056. Standard Test for Soils Investigation and Testing-Granulometric Analysis-Dry Sieving method after Washing. 1996.
- NF P 94-057. Standard Test for Soils Investigation and Testing-Granulometric Analysis-Hydrometer method. 1992.
- NF P 94-093. Standard Test for Soils Investigation and Testing-Determination of the Compaction Characteristics of a Soil-Standard Proctor test-Modified Proctor test. 1999.
- Ng CWW, Yung SY. Determination of the anisotropic shear stiffness of an unsaturated decomposed soil. *Géotechnique* 2008;58(1):23-35.
- Ng CWW, Xu J, Yung SY. Effects of wetting-drying and stress ratio on anisotropic stiffness of an unsaturated soil at very small strains. *Can Geotech J* 2009;46(9):1062-1076.
- Ng CWW, Baghbanrezvan S, Sadeghi H, Zhou C, Jafarzadeh F. Effect of specimen preparation techniques on dynamic properties of unsaturated fine-grained soil at high suctions. *Can Geotech J* 2017;54(9):1310-1319.

- Noorany I. Phase relations in marine soils. *J Geotech Eng* 1984;110(4):539-543.
- Ravi K, Rao SM. Influence of infiltration of sodium chloride solutions on SWCC of compacted bentonite–sand specimens. *Geotech Geol Eng* 2013;31(4):1291-1303.
- Reitemeier RF. Effect of moisture content on the dissolved and exchangeable ions of soils of arid regions. *Soil Sci* 1946;61(3):195-214.
- Romero E, Della Vecchia G, Jommi C. (2011). An insight into the water retention properties of compacted clayey soils. *Géotechnique*. 2011;61(4):313-328.
- Romero E. A microstructural insight into compacted clayey soils and their hydraulic properties. *Eng. Geol.* 2013;165:3-19.
- Russo G, Modoni G. Fabric changes induced by lime addition on a compacted alluvial soil. *Géotechnique Lett* 2013;3(2):93-97.
- Sarkar G, Siddiqua S. Effect of fluid chemistry on the microstructure of light backfill: An X-ray CT investigation. *Eng Geol* 2016;202:153-162.
- Shariatmadari N, Salami M, Fard MK. Effect of inorganic salt solutions on some geotechnical properties of soil-bentonite mixtures as barriers. *Int J Civ Eng* 2011;9 (2):103-110.
- Siddiqua S, Blatz J, Siemens J. Evaluation of the impact of pore fluid chemistry on the hydromechanical behaviour of clay-based sealing materials. *Can Geotech J* 2011;48(2): 199-213.
- Sreedeeep S, Singh DN. Critical review of the methodologies employed for soil suction measurement. *Int J Geomech* 2011;11(2):99-104.
- Sridharan A, Jayadeva MS. Double layer theory and compressibility of clays. *Géotechnique* 1982;32(2):133-144.
- Sridharan A, Prakash K. Percussion and cone methods of determining the liquid limit of soils: controlling mechanisms. *Geotech Test J* 2000;23(2):236-244.
- Sridharan A, AEl-Shafei A, Miura N. Mechanisms controlling the undrained strength behaviour of remolded Ariake marine clays. *Mar Georesour Geotechnol* 2002;20(1):21-50.
- Tang AM, Vu MN, Cui YJ. Effects of the maximum soil aggregates size and cyclic wetting-drying on the stiffness of a lime-treated clayey soil. *Géotechnique* 2011;61(5):421-429.
- Tatsuoka F. Compaction characteristics and physical properties of compacted soil controlled by the degree of saturation. *Proc. 15th Pan-American Conf. on SMGE & 6th IC on Deformation Characteristics of Geomaterials, Buenos Aires* 2015:40-76.
- Tatsuoka F, Correia AG. Importance of controlling the degree of saturation in soil compaction linked to soil structure design. *Trans Geotech* 2018;17:3-27.
- Thyagaraj T, Salini U. Effect of pore fluid osmotic suction on matric and total suctions of compacted clay. *Géotechnique* 2015;65(11):952-960.
- Tiwari B, Tuladhar GR, Marui H. Variation in residual shear strength of the soil with the salinity of pore fluid. *J Geotech Geoenviron Eng* 2005;131(12):1445-1456.
- Truong QH, Lee C, Kim YU, Lee JS. Small strain stiffness of salt-cemented granular media under low confinement. *Géotechnique* 2012;62(10):949-953.
- Wan AWL, Gray MN, Graham J. On the relations of suction, moisture content and soil structure in compacted clays. *Proc. 1st Int. Conf. on Unsaturated Soils, Paris. Vol. 1. Balkema/Presses des Ponts et Chaussées.* 1995.

- Wang YJ, Benahmed N, Cui YJ, Tang AM. A novel method for determining the small-strain shear modulus of soil using the bender elements technique. *Can Geotech J* 2017;54(2): 280-289.
- Wang YJ, Cui YJ, Benahmed N, Tang AM, Duc M. Changes of small strain shear modulus and suction for a lime-treated silt during curing. *Géotechnique* 2020;70(3):276-280.
- Warkentin BP, Yong RN. Shear strength of montmorillonite and kaolinite related to interparticle forces. *Proc. 9th Nation. Conf. Clays Clay Miner.* Pergamon, 1962:210-218.
- Witteveen P, Ferrari A, Laloui L. An experimental and constitutive investigation on the chemo-mechanical behaviour of a clay. *Géotechnique* 2013;63(3):244-255.
- Yılmaz G, Yetimoglu T, Arasan S. Hydraulic conductivity of compacted clay liners permeated with inorganic salt solutions. *Waste Manag Res* 2008;26(5):464-473.
- Ying Z, Duc M, Cui YJ, Benahmed N. Salinity assessment for salted soil considering both dissolved and precipitated salts. *Geotech Test J* 2020a;44(1), Online DOI: 10.1520/GTJ20190301.
- Ying, Z., Cui, Y. J., Duc, M., Benahmed, N., Bessaies-Bey. H. & Chen, B. Salinity effect on the liquid limit of soils. *Acta Geotechnica.* 2020b. Online, DOI: 10.1007/s11440-020-01092-7.
- Zhang FY, Wang GH, Kamai T, Chen WW, Zhang DX, Yang J. Undrained shear behaviour of loess saturated with different concentrations of sodium chloride solution. *Eng Geol* 2013a;155:69-79.
- Zhang DW, Fan LB, Liu SY, Deng YF. Experimental investigation of unconfined compression strength and stiffness of cement treated salt-rich clay. *Mar Georesour Geotechnol* 2013b;31(4):360-374.
- Zhang TW, Cui YJ, Lamas-Lopez F, Calon N, Costa D'Aguiar S. Compacted soil behaviour through changes of density, suction, and stiffness of soils with remoulding water content. *Can Geotech J* 2018;55(2):182-190.
- Zhang Y, Ye WM, Chen YG, Chen B. Impact of NaCl on drying shrinkage behavior of low-plasticity soil in earthen heritages. *Can Geotech J* 2017;54(12):1762-1774.